

Comparison of solid-state thermionic refrigeration with thermoelectric refrigeration

Marc D. Ulrich^{a)} and Peter A. Barnes
206 Allison Laboratory, Auburn University, Alabama 36849-5311

Cronin B. Vining
ZT Services, 2203 Johns Circle, Auburn, Alabama 36830-7113

(Received 27 December 2000; accepted for publication 26 April 2001)

A theoretical analysis of single-barrier thermionic emission cooling in semiconducting materials is performed using Fermi–Dirac statistics. Both maximum cooling and coefficient of performance are evaluated. It is shown that the performance of a thermionic refrigerator is governed by the same materials factor as thermoelectric devices. For all known materials, single-barrier thermionic refrigeration is less effective and less efficient than thermoelectric refrigeration. © 2001 American Institute of Physics. [DOI: 10.1063/1.1380996]

I. INTRODUCTION

The motivation to study solid-state thermionic refrigeration has been the potential for substantial improvement in room-temperature thermoelectric performance. The realization of more effective cooling and energy conversion in thermoelectrics requires the discovery of new materials. However, it is possible that new types of devices may outperform thermoelectric devices in known materials. A thermionic emission cooler has been proposed to be such a device.¹ It is the purpose of this manuscript to develop a robust theory of solid-state thermionic refrigeration and to compare the maximum cooling and coefficient of performance (COP) of thermionic refrigeration with standard thermoelectric refrigeration.

Figure 1 shows a band diagram of a thermionic emission cooler with an applied bias. The emitter and collector consist of either metal or a heavily doped semiconductor. The barrier is made of a less heavily doped semiconductor and is made thin enough so that electrons travel ballistically through the barrier layer. The principle of cooling is based on the Peltier effect. Electrons passing through the barrier layer from the emitter to the collector cause cooling at the emitter–barrier junction and heating at the barrier–collector junction.

There are two primary differences between a thermionic device and a thermoelectric device. Both differences are the result of ballistic transport through the barrier region. First, The electrical and heat currents through a thermionic device are nonlinear with respect to both the voltage and temperature difference. Second, there is no joule heating in the barrier layer of an ideal thermionic device.

A more rigorous theoretical model of thermionic emission cooling must be developed for several reasons. Most importantly, Shakouri *et al.* have recognized that the Boltzmann approximation on which all current models are based does not accurately describe an optimally designed thermionic emission cooler.² Second, it has been determined in this

research that the correct parameter controlling carrier transport across semiconductor heterojunction interfaces has not been used in the modeling of thermoelectricity. Third, a model including the analysis of both maximum cooling and coefficient of performance has not been developed.

II. THERMIONIC THEORY

Ideally, current in a thermionic device is governed only by the heterojunctions on either side of the barrier layer. It is assumed that there is no band bending at the interfaces. This simplification is justified because, as it will be seen later, the necessary doping for thermionic refrigeration is degenerate and thus the depletion widths will be small. Also, it is theoretically possible to engineer a flatband junction involving a quaternary material (such as InGaAs/InGaAsP) by adjusting the chemical composition and the doping levels to match the work functions of the two materials.

Electrical current over a heterojunction barrier is usually described by the Richardson equation. This is an approximation equivalent to replacing Fermi–Dirac (FD) statistics with Boltzmann statistics and is valid if the energy barrier to the flow of electrons is sufficiently large ($\geq 3kT$). The optimum energy barrier for thermionic refrigeration lies outside this region of validity.² To consider all possible barriers, FD statistics are used in this model.

The general equations for electrical current density J_E and heat current density J_Q over a heterojunction boundary are^{3,4}

$$J_E = \int_{-\infty}^{\infty} \int_{-\infty}^{\infty} \int_{p_x^{\text{free}}}^{\infty} f(p)g(p)qv_x dp_x dp_y dp_z, \quad (1.1)$$

$$J_Q = \int_{-\infty}^{\infty} \int_{-\infty}^{\infty} \int_{p_x^{\text{free}}}^{\infty} f(p)g(p)[\epsilon(p) - \epsilon_f]v_x dp_x dp_y dp_z, \quad (1.2)$$

where $f(p)$ is the FD distribution function in momentum space, $g(p)$ is the density of states in momentum space, q is the electron charge, v_x is the electron velocity in the x direction, i.e., the direction of transport, $\epsilon(p)$ is the electron ki-

^{a)}Present address: Department of Physics, North Carolina State University, Raleigh, NC 27695-7518; electronic mail: mdulrich@unity.ncsu.edu

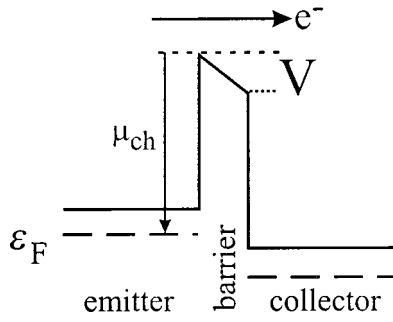


FIG. 1. Band diagram of a thermionic emission cooler with an applied bias.

netic energy, ϵ_f is the Fermi energy measured from the conduction-band edge of the emitting material, and the range of integration is over all momentum space for electrons with a momentum in the direction perpendicular to the interface greater than p_x^{free} , the momentum necessary to surmount the barrier.

The solutions to the electrical and heat current density in terms of FD integrals are

$$J_E = A^* T^2 \mathcal{F}_1(\eta), \quad (1.3)$$

$$J_Q = A^* T^2 \frac{kT}{q} [2\mathcal{F}_2(\eta) - \eta \mathcal{F}_1(\eta)]. \quad (1.4)$$

The FD integrals, $\mathcal{F}_n(\eta)$, are defined in the Appendix. A^* is the effective Richardson constant and is defined as

$$A^* = \frac{4\pi q m^* k^2}{h^3}. \quad (1.5)$$

T is the temperature at the heterojunction, k is the Boltzmann constant, m^* is the electron effective mass, h is Planck's constant, and η is defined as

$$\eta = \frac{q\mu_{\text{ch}}}{kT} = \frac{\epsilon_f - \epsilon_C^{\text{barrier}}}{kT}, \quad (1.6)$$

where μ_{ch} is a chemical potential as shown in Fig. 1, and $\epsilon_C^{\text{barrier}}$ is the conduction-band edge of the barrier. If there is no band bending at the heterojunctions, then η is equivalent to the reduced Fermi energy of the barrier material.

A chemical potential in the barrier of a thermionic device can only be defined when there is an equilibrium FD distribution of electrons in the barrier. Because transport through the barrier of a thermionic device is strictly ballistic, the distribution will not be FD, and a chemical potential cannot be defined in the barrier region. Thus, the variable μ_{ch} is strictly defined outside the barrier as in Eq. (1.6) and in Fig. 1. However, because this corresponds to the chemical potential of the equivalent bulk barrier material, μ_{ch} will be referred to as the chemical potential and η will be referred to as the reduced Fermi energy.

It is a crucial point that the chemical potential is responsible for determining the currents over a heterojunction boundary. In the case of a metal–semiconductor heterojunction, the barrier height defined by Richardson⁵ is the same as the chemical potential of the semiconductor if there is no band bending. However, it has been incorrectly assumed that

for a semiconductor–semiconductor heterojunction boundary that the energy-band offset, and not the chemical potential, controls the currents.^{6,7}

In 1979, Wu and Yang presented a detailed derivation of the electrical currents over a semiconductor heterojunction interface.⁸ Their results included the effects of band bending at the interface and assumed the Richardson approximation. Their results agree with the result determined here: that the parameter controlling the flow of carriers is measured from the Fermi level of the emitting material.

In a thermionic refrigerator, two heterojunctions govern the currents. An applied forward bias lowers the electron energy on the collector side and suppresses current from the collector toward the emitter. The fundamental charge q is taken to be a positive value and the electrical current density is positive for the flow of electrons from the emitter to the collector. Thermal conduction through the lattice of the barrier is also considered. The electrical and heat current densities leaving the emitter of a thermionic refrigerator for forward bias are

$$J_E = A^* T_C^2 \mathcal{F}_1(\eta) - A^* T_H^2 \mathcal{F}_1\left(\eta \frac{T_C}{T_H} - \frac{qV}{kT_H}\right), \quad (1.7)$$

$$J_Q = A^* T_C^3 \frac{k}{q} [2\mathcal{F}_2(\eta) - \eta \mathcal{F}_1(\eta)] - A^* T_H^3 \frac{k}{q} \left[2\mathcal{F}_2\left(\eta \frac{T_C}{T_H} - \frac{qV}{kT_H}\right) - \eta \frac{T_C}{T_H} \mathcal{F}_1\left(\eta \frac{T_C}{T_H} - \frac{qV}{kT_H}\right) \right] - \frac{\kappa_l}{d} \Delta T, \quad (1.8)$$

where T_C is the temperature at the emitter–barrier junction (the cold side), T_H is the temperature at the barrier–collector junction (the hot side), V is the applied voltage, κ_l is the lattice thermal conductivity of the barrier material, d is the width of the barrier, and $\Delta T = T_H - T_C$. Energy balance has been accounted for in Eqs. (1.7) and (1.8). In determining Eqs. (1.7) and (1.8), it has been assumed that the chemical potential and the lattice thermal conductivity are independent of the temperature.

From these two fundamental thermionic equations the maximum cooling and COP will be determined. To make a comparison with thermoelectrics, the figure of merit for a thermoelectric device must first be carefully examined.

III. THERMOELECTRIC FIGURE OF MERIT

Usually, the nondegenerate solution is sufficient to determine the figure of merit for thermoelectrics. However, since a careful comparison with thermionics, which uses FD statistics, is going to be made, it is profitable to use FD statistics for thermoelectrics as well.

The parameter characterizing thermoelectric performance is the figure of merit Z , or the dimensionless figure of merit ZT . The general equation for ZT is

$$ZT = \frac{\sigma S^2 T}{\kappa_l + \kappa_e} = \frac{S^2}{\frac{\kappa_l}{\sigma T} + L}, \quad (2.1)$$

where S is the Seebeck coefficient, σ is the electrical conductivity, κ_e is the electronic contribution to the thermal conductivity, and L is the Lorenz number defined as

$$L = \frac{\kappa_e}{\sigma T}. \quad (2.2)$$

The three parameters, σ , S , and L are determined using the Boltzmann equation to describe electron transport through the thermoelectric device. To compare thermionic and thermoelectric results a correlation must be made between the assumptions made in each theory. This requires a discussion of scattering as it directly affects the three parameters discussed above. The simplified model of electron scattering used in thermoelectric theory is to assume that the relaxation time can be expressed as

$$\tau = \tau_0 E^r, \quad (2.3)$$

where τ_0 is a constant, E is the energy of an electron, and r is a scattering parameter. In the thermionic device, it has been assumed that all electrons travel through the barrier ballistically and are then scattered in the collector. If a maximum barrier width of one mean-free path is chosen, the mean-free path of all electrons must be independent of their energy. The classical relationship between the mean-free path λ and the relaxation time τ is

$$\lambda = \tau v, \quad (2.4)$$

where v is the average velocity of the electrons. Since the velocity will be proportional to $E^{1/2}$, the mean-free path of all electrons will be independent of their energy if the scattering parameter r is chosen to be $-1/2$. This corresponds to a scattering model in which acoustic phonon scattering is dominant.⁹

Using this scattering model, the thermoelectric parameters that determine ZT are¹⁰

$$S = \frac{k}{q} \left(\eta - 2 \frac{\mathcal{F}_1(\eta)}{\mathcal{F}_0(\eta)} \right), \quad (2.5)$$

$$L = \frac{k^2}{q^2} \left[6 \frac{\mathcal{F}_2(\eta)}{\mathcal{F}_0(\eta)} - 4 \frac{\mathcal{F}_1(\eta)^2}{\mathcal{F}_0(\eta)^2} \right], \quad (2.6)$$

$$\sigma = \frac{16\sqrt{2}\pi}{3} q^2 \frac{\sqrt{m^*}}{h^3} \tau_0 k T \mathcal{F}_0(\eta). \quad (2.7)$$

The electrical conductivity can also be obtained using

$$\sigma = nq\mu = 2q\mu \left(\frac{2\pi m^* kT}{h^2} \right)^{3/2} \mathcal{F}_{1/2}(\eta). \quad (2.8)$$

By equating both forms, the mobility at any doping can be defined in terms of the nondegenerate mobility μ_0 and the reduced Fermi energy:

$$\mu = \mu_0 \frac{\mathcal{F}_0(\eta)}{\mathcal{F}_{1/2}(\eta)}. \quad (2.9)$$

Utilizing this relationship the functional form of the electrical conductivity is

$$\sigma = 2q\mu_0 \left(\frac{2\pi m^* kT}{h^2} \right)^{3/2} \mathcal{F}_0(\eta). \quad (2.10)$$

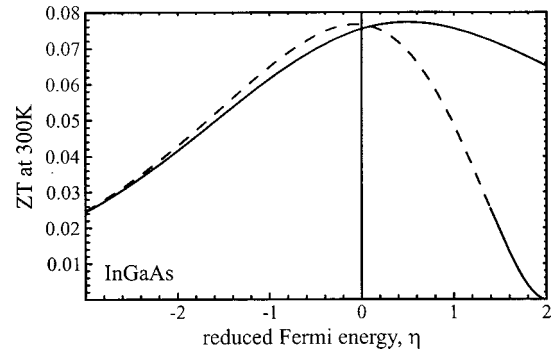


FIG. 2. Comparison of the dimensionless figure of merit based on the Boltzmann approximation (dashed) and on Fermi–Dirac statistics (solid).

With this definition of the electrical conductivity, the final term in the dimensionless figure of merit becomes

$$\frac{\kappa_l}{\sigma T} = \frac{k^2}{q^2} \beta^{-1} [\mathcal{F}_0(\eta)]^{-1}. \quad (2.11)$$

All of the material characteristics are contained in β , which is called the materials parameter,¹¹

$$\beta = \frac{4\pi\sqrt{2}\pi k^{3.5}}{qh^3} \left(\frac{\mu_0(m^*)^{1.5} T^{2.5}}{\kappa_l} \right). \quad (2.12)$$

Using Eqs. (2.5), (2.6), and (2.11), the figure of merit for a thermoelectric device is determined by the materials parameter β and the reduced Fermi energy η . This will be used when thermionics are compared with thermoelectrics.

To show the importance of using Fermi–Dirac statistics consider Fig. 2, which shows the dimensionless figure of merit evaluated using FD statistics and using the nondegenerate solution as a function of the reduced Fermi energy. The materials parameter used in this figure is $\beta=0.02$, which corresponds to the InGaAs material. The maximum is in the degenerate region where it is necessary to consider Fermi–Dirac statistics. Though the nondegenerate solution fails to evaluate the optimum reduced Fermi energy accurately, the maximum figure of merit for both solutions is nearly the same. Correspondence between the two solutions is also seen as the reduced Fermi energy becomes more negative where the Boltzmann approximation is valid.

IV. THERMIONIC MAXIMUM COOLING

Maximum cooling in a thermionic device occurs when the heat load is zero. If the device is driven to saturation (i.e., current densities are maximized and independent of applied bias), then the heat current and electrical current are maximized. At saturation, an analytical solution for the temperature difference is determined by setting Eq. (1.8) to zero:

$$\Delta T_{\max} = \frac{d}{\kappa_l} A^* T_C^2 \frac{kT_C}{q} [2\mathcal{F}_2(\eta) - \eta\mathcal{F}_1(\eta)]. \quad (3.1)$$

To determine an upper limit to the cooling, the barrier width is set to one mean-free path. Because transport is not truly ballistic at this width, it is certain that the cooling cannot be more than the results obtained with this choice. The mean-

free path λ can be expressed in terms of the effective mass m^* and the bulk mobility μ of electrons in the barrier material:

$$\lambda = \sqrt{2m^*kT}\mu/q. \quad (3.2)$$

Thus,

$$\Delta T_{\max} = \frac{4\pi\sqrt{2}(m^*)^{1.5}(kT_C)^{3.5}\mu/q}{\kappa_l h^3} [2\mathcal{F}_2(\eta) - \eta\mathcal{F}_1(\eta)]. \quad (3.3)$$

A materials parameter for thermionic refrigeration is

$$\beta_{TI} = \frac{4\pi\sqrt{2}k^{3.5}}{qh^3} \left(\frac{\mu(m^*)^{1.5}}{\kappa_l} T_C^{2.5} \right). \quad (3.4)$$

The maximum cooling in terms of this parameter is

$$\Delta T_{\max} = \beta_{TI} T_C [2\mathcal{F}_2(\eta) - \eta\mathcal{F}_1(\eta)]. \quad (3.5)$$

The mobility used in the thermionic materials parameter is the degenerate mobility of the bulk barrier material. To ensure that a careful comparison with thermoelectrics can be made, the degenerate mobility is related to the nondegenerate mobility just as it is done for thermoelectrics using Eq. (2.9).

The resulting relationship between the thermionic and thermoelectric materials parameters is

$$\frac{\beta_{TI}}{\beta} = \frac{1}{\sqrt{\pi}} \frac{\mathcal{F}_0(\eta)}{\mathcal{F}_{1/2}(\eta)}. \quad (3.6)$$

With this, the maximum cooling can be written in terms of the thermoelectric materials parameter

$$\Delta T_{\max} = \frac{1}{\sqrt{\pi}} \beta [2\mathcal{F}_2(\eta) - \eta\mathcal{F}_1(\eta)] \frac{\mathcal{F}_0(\eta)}{\mathcal{F}_{1/2}(\eta)} T_C. \quad (3.7)$$

Thus, maximum cooling for a thermionic device depends upon the same materials parameter as a thermoelectric device.

In a thermoelectric device, the dimensionless figure of merit is related to the maximum cooling according to

$$ZT = 2(\Delta T_{\max}/T). \quad (3.8)$$

It is convenient to utilize this to determine an effective figure of merit for a thermionic device operating at maximum cooling:

$$ZT_{TI} = \frac{2}{\sqrt{\pi}} \beta [2\mathcal{F}_2(\eta) - \eta\mathcal{F}_1(\eta)] \frac{\mathcal{F}_0(\eta)}{\mathcal{F}_{1/2}(\eta)}. \quad (3.9)$$

Figure 3 compares the cooling for a thermionic device with an InGaAs barrier layer and an InGaAs thermoelectric device as a function of the reduced Fermi energy. The effective mass ratio of electrons in InGaAs is $m^*/m_0 = 0.041$.¹² The nondegenerate mobility is taken to be $13\,800\text{ cm}^2/\text{V s}$.¹³ It is assumed that the thermal conductivity corresponds to the bulk value of 0.05 W/cm K .¹⁴ This results in a materials parameter for InGaAs of $\beta = 0.02$. Figure 4 shows the same comparison for Bi_2Te_3 . At room temperature the effective mass ratio of electrons in Bi_2Te_3 is $m^*/m_0 = 0.58$, the mobility is $1200\text{ cm}^2/\text{V s}$, and the lattice thermal conductivity of bulk material is 0.015 W/cm K .¹⁵ Thus, the materials param-

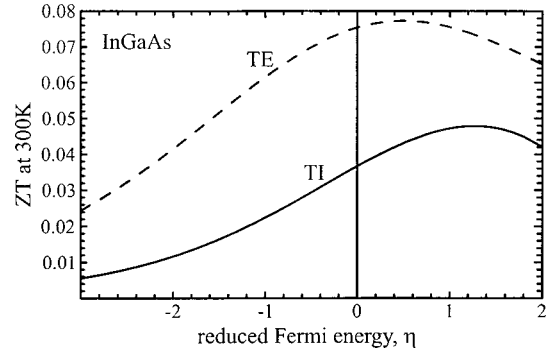


FIG. 3. Comparison of the thermionic effective figure of merit (solid) and thermoelectric figure of merit (dashed) for InGaAs at room temperature.

eter for Bi_2Te_3 is $\beta = 0.316$. In both materials, thermionic refrigeration does not perform as well as the thermoelectric refrigeration.

To make a comparison of the effective figures of merit as a function of the materials parameter, both must be optimized with respect to the reduced Fermi energy. For a thermoelectric device, the optimum reduced Fermi energy is determined numerically. For a thermionic device, the optimum reduced Fermi energy is independent of the material and is found by maximizing the function

$$[2\mathcal{F}_2(\eta) - \eta\mathcal{F}_1(\eta)] \frac{\mathcal{F}_0(\eta)}{\mathcal{F}_{1/2}(\eta)}. \quad (3.10)$$

The optimum reduced Fermi energy is found numerically to be $\eta_{\text{opt}} = 1.27$. This optimum corresponds to the Fermi energy residing 1.27 times the thermal energy above the conduction-band edge of the barrier confirming that FD statistics are necessary for the analysis of thermionic refrigeration.

Figure 5 plots the maximum figures of merit as a function of the materials parameter. The range of the materials parameter is from 0 to 0.5. This spans the full range of known materials and further so that possible undiscovered materials may also be considered. Two lines are also provided to show the materials parameters for InGaAs and Bi_2Te_3 . For the full range of materials considered, the thermionic device does not perform as well as the thermoelectric device.

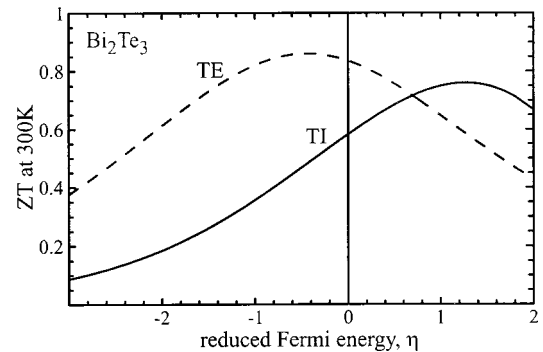


FIG. 4. Comparison of the thermionic effective figure of merit (solid) and thermoelectric figure of merit (dashed) for Bi_2Te_3 at room temperature.

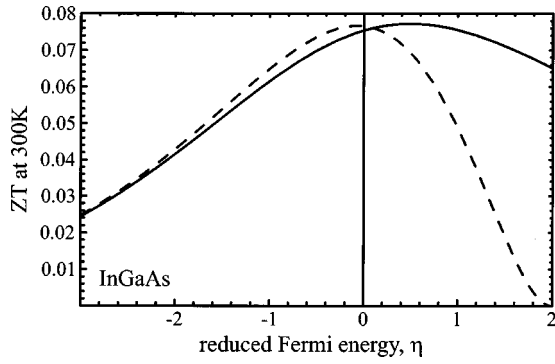


FIG. 5. Maximum effective figure of merit for a thermionic (solid) and the maximum figure of merit of a thermoelectric (dashed) as a function of the materials parameter.

V. THERMIONIC COEFFICIENT OF PERFORMANCE

The COP is the ratio of the heat removed from the cold side (the emitter) to the electrical power input to the device:

$$COP = \frac{J_Q}{J_E V}. \tag{4.1}$$

This is not optimized at saturation of the currents so the complete solutions for the current densities found in Eqs. (1.7) and (1.8) must be considered. To clarify the complex equation, two dimensionless functions, *fe* and *fq*, are defined to represent the normalized electrical and heat current densities due to electrons:

$$J_E = A * T_C^2 fe(\eta, V, T_C, \Delta T). \tag{4.2}$$

and

$$J_Q = \frac{k}{q} A * T_C^3 fq(\eta, V, T_C, \Delta T) - \frac{\kappa_l}{d} \Delta T. \tag{4.3}$$

Again, taking the width of the barrier to be equal to the electron mean-free path, the COP is

$$COP = \frac{k T_C}{q V} \frac{fq(\eta, V, T_C, \Delta T) - \frac{q h^3 \kappa_l}{4 \pi \sqrt{2} (m^*)^{1.5} k^{3.5} T_C^{2.5} \eta} \frac{\Delta T}{T_C}}{fe(\eta, V, T_C, \Delta T)}. \tag{4.4}$$

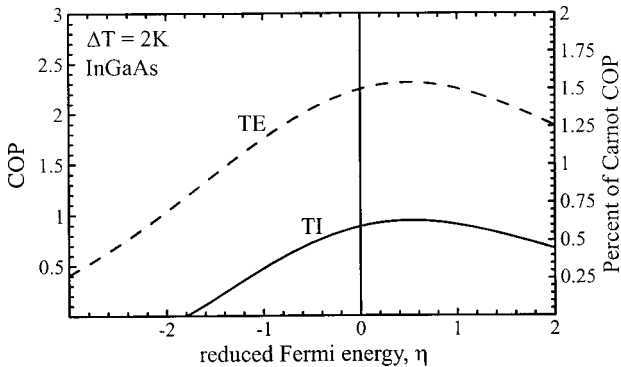


FIG. 6. Coefficient of performance for a thermionic device with an InGaAs barrier (solid) and an InGaAs thermoelectric device (dashed) at room temperature and a temperature difference of $\Delta T=2$ K as a function of the reduced Fermi energy.

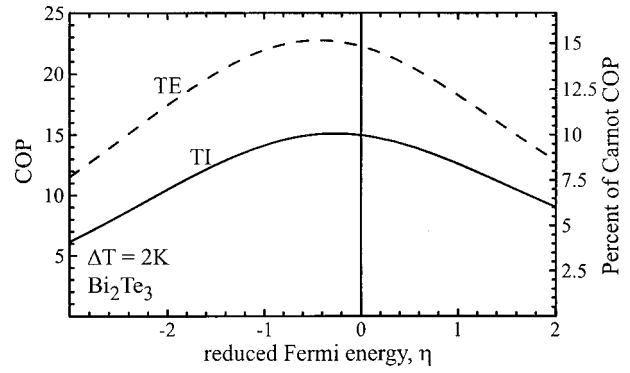


FIG. 7. Coefficient of performance for a thermionic device with a Bi_2Te_3 barrier (solid) and a Bi_2Te_3 thermoelectric device (dashed) at room temperature and a temperature difference of $\Delta T=2$ K as a function of the reduced Fermi energy.

This can also be written in terms of the thermoelectric materials parameter,

$$COP = \frac{k T_C}{q V} \frac{fq(\eta, V, T_C, \Delta T) - \frac{\sqrt{\pi} \Delta T}{\beta} \frac{F_{1/2}(\eta)}{T_C} \frac{F_0(\eta)}}{fe(\eta, V, T_C, \Delta T)}. \tag{4.5}$$

Thus, the COP is also dependent upon the same materials parameter as for a thermoelectric device.

The analysis of the COP is done by numerically optimizing the voltage and by assuming a temperature difference of $\Delta T=2$ K. A temperature difference of $\Delta T=2$ K is chosen so that the COP is greater than zero for nearly all values of the materials parameter. Figure 6 shows the maximum COP for a thermionic device and a thermoelectric device using InGaAs as a function of the reduced Fermi energy at room temperature for a temperature difference of $\Delta T=2$ K. Figure 7 shows the same comparison for Bi_2Te_3 . For both materials, the thermoelectric performs better.

Figure 8 shows the maximized COP for both a thermionic and thermoelectric as a function of the materials parameter ranging from 0 to 0.5. The thermoelectric device is more efficient than the thermionic device in all known and unknown materials.

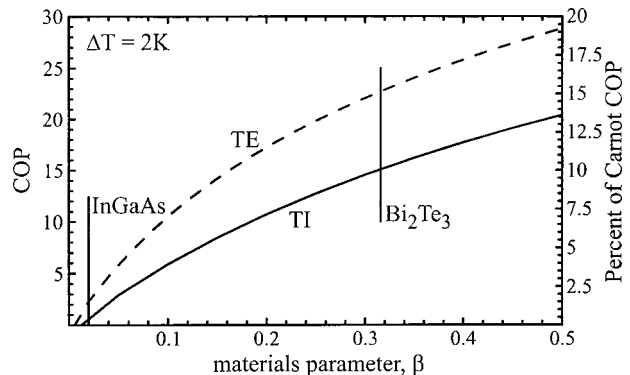


FIG. 8. Coefficient of performance for a thermionic device (solid) and a thermoelectric device (dashed) at room temperature and a temperature difference of $\Delta T=2$ K as a function of the materials parameter.

VI. DISCUSSION AND CONCLUSIONS

In 1999, Vining and Mahan determined a materials parameter for thermionics in the Boltzmann regime and in the linear limit.¹⁶ Their result for the ratio of the thermionic materials parameter β_{TI} to thermoelectric materials parameter β is

$$\frac{\beta_{TI}}{\beta} = \frac{d}{\lambda \sqrt{\pi}}, \quad (5.1)$$

thus concluding that the thermoelectric device always performs better than a thermionic device as the barrier width d cannot be larger than one mean-free path λ . In the model presented in this article, the relationship between the materials parameters [Eq. (3.6)] is determined using Fermi–Dirac statistics and apart from linearization. In this model, the barrier width d has been taken to be exactly one mean-free path and the factor of π is also present. In the Boltzmann regime, all orders of the Fermi–Dirac integrals reduce to an exponential and the ratio in Eq. (3.6) becomes unity. Thus, these results agree exactly with those obtained by Vining and Mahan.

A comparison of vacuum thermionic emission refrigeration and thermoelectric refrigeration for projected devices has been provided by Nolas and Goldsmid.¹⁷ Their results show that a vacuum thermionic refrigerator with an electrode having a work function of $\phi=0.3$ eV would be superior to thermoelectric refrigeration in a material with a dimensionless figure of merit of $ZT=4$. This is due to the superior transport properties of a vacuum (for example, an effective mass ratio of $m^*/m_0=1$) and that the transport of heat to the cold junction due to radiation is less than that due to a lattice. Room-temperature refrigeration in thermionic emission devices cannot be accomplished with today's technology and solid-state thermionic refrigeration is a valid consideration. Interestingly, though, when a material replaces the vacuum, thermionic refrigeration is limited by exactly the same materials parameter that is found in thermoelectric refrigeration.

We have shown in this article that a solid-state thermionic device and thermoelectric device depend upon the same materials parameter though they do not depend upon that parameter in the same way. A similar result was also obtained by Shakouri using a less complex model for maximum cooling.¹⁸ This result should be expected. The same physical phenomena that cause cooling in a thermoelectric device cause cooling in a thermionic device. The only differences between a thermionic and thermoelectric is that the thermionic device lacks joule heat and is nonlinear. These may affect the cooling and efficiency, but should not affect the relationship between the characteristics of the material used in the device.

Assumptions that are similar to those made in standard thermoelectric theory have been made in this model also. It has been assumed that certain material parameters of the barrier material are independent of temperature: the lattice thermal conductivity, the mobility, and the chemical potential. The difference between this and thermoelectrics is that in thermoelectrics it is assumed that the Seebeck coefficient (proportional to $2 - \eta$) is independent of temperature. This is

similar, but not quite the same as assuming that the chemical potential is independent of temperature as $\eta=q\mu_{ch}/kT$.

There are other assumptions and simplifications that have been made in this model. It has been assumed that there is no quantum reflection at the heterojunctions. It has also been assumed that all electrons that enter the barrier region will traverse the barrier and do so without scattering. All of these are overestimations and thus provide an upper bound to the cooling ability of an ideal, single-barrier, solid-state thermionic device.

Thus, for all known materials, thermoelectric refrigeration is more effective and efficient than single-barrier solid-state thermionic refrigeration.

APPENDIX

The Fermi–Dirac integral of order n is defined as

$$\mathcal{F}_n(\eta) = \frac{1}{\Gamma(n+1)} \int_0^\infty \frac{\epsilon^n d\epsilon}{\exp(\epsilon - \eta) + 1}. \quad (A1)$$

FD integrals are actually a part of the family of functions called the polylogarithms. The polylogarithm can be defined in the following form:¹⁹

$$\text{Li}_n(z) = \frac{1}{\Gamma(n)} \int_0^\infty \frac{\epsilon^{n-1} d\epsilon}{z^{-1} \exp(\epsilon) - 1}, \quad \text{Re } n > 0. \quad (A2)$$

The general relationship between the FD integrals and the polylogarithms is

$$\mathcal{F}_n(\eta) = -\text{Li}_{n+1}[-\exp(\eta)]. \quad (A3)$$

The polylogarithms are highly useful for solving FD integrals because they are built into standard mathematical packages such as MATHEMATICA²⁰ and MAPLE.²¹ Such packages provide extremely fast and efficient calculation of the polylogarithms to any prescribed accuracy. The calculations in this research were accomplished using MATHEMATICA.

Other authors, such as Reser²² and Lee^{23–25} have also noted the usefulness of polylogarithms in calculating FD integrals.

¹G. D. Mahan and L. M. Woods, Phys. Rev. Lett. **80**, 4016 (1998).

²A. Shakouri, E. Y. Lee, D. L. Smith, V. Narayanamurti, and J. E. Bowers, Microscale Thermophys. Eng. **2**, 37 (1998).

³R. A. Smith, *Semiconductors* (Cambridge University, Cambridge, 1964), p. 110.

⁴N. W. Ashcroft and N. D. Mermin, *Solid State Physics* (Harcourt Brace College, Fort Worth, TX, 1976), p. 254.

⁵O. W. Richardson, Philos. Mag. **23**, 594 (1912).

⁶T. Zeng and G. Chen, in Proceedings of the 18th International Conference on Thermoelectrics (1999), p. 590.

⁷A. Shakouri and J. E. Bowers, Appl. Phys. Lett. **71**, 1234 (1997).

⁸C. M. Wu and E. S. Yang, Solid-State Electron. **22**, 241 (1979).

⁹B. R. Nag, in *Electron Transport in Compound Semiconductors*, Springer Series in Solid-State Sciences, Vol. 11 (Springer, New York, 1980), p. 174.

¹⁰H. J. Goldsmid, *Electronic Refrigeration* (Pion, London, 1986), p. 59.

¹¹H. J. Goldsmid, *Electronic Refrigeration* (Pion, London, 1986), p. 58.

¹²O. Madelung, *Landolt-Bornstein New Series III/22a* (Springer, Berlin, 1987), p. 143.

¹³O. Madelung, *Landolt-Bornstein New Series III/22a* (Springer, Berlin, 1987), p. 144.

¹⁴F. D. Rossi, Solid-State Electron. **11**, 833 (1968).

¹⁵H. J. Goldsmid, *Electronic Refrigeration* (Pion, London, 1986), p. 96.

¹⁶C. B. Vining and G. D. Mahan, J. Appl. Phys. **86**, 6852 (1999).

¹⁷G. S. Nolas and H. J. Goldsmid, J. Appl. Phys. **85**, 4066 (1999).

- ¹⁸A. Shakouri and C. LaBounty, in Proceedings of the 18th International Conference on Thermoelectrics (1999), p. 35.
- ¹⁹L. Lewin, *Polylogarithms and Associated Functions* (North-Holland, New York, 1981), p. 236.
- ²⁰S. Wolfram, *The Mathematica Book* (Cambridge University, New York, 1999), p. 1.
- ²¹Waterloo Maple Inc., 57 Erb Street West, Waterloo, Ontario, Canada N2L 6C2, www.maplesoft.com
- ²²B. I. Reser, *J. Phys.: Condens. Matter* **8**, 3151 (1996).
- ²³M. H. Lee, *J. Math. Phys.* **36**, 1217 (1995).
- ²⁴M. H. Lee, *Phys. Rev. E* **53**, 5488 (1996).
- ²⁵M. H. Lee, *Phys. Rev. E* **54**, 946 (1996).